

# Surfactant Removal for Colloidal Nanoparticles from Solution Synthesis: The Effect on Catalytic Performance

Dongguo Li,<sup>†,‡</sup> Chao Wang,<sup>†</sup> Dusan Tripkovic,<sup>†</sup> Shouheng Sun,<sup>\*,‡</sup> Nenad M. Markovic,<sup>†</sup> and Vojislav R. Stamenkovic<sup>\*,†</sup>

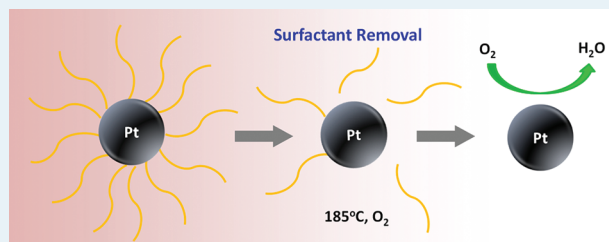
<sup>†</sup>Materials Science Division, Argonne National Laboratory, Argonne, Illinois 60439, United States

<sup>‡</sup>Department of Chemistry, Brown University, Providence, Rhode Island 02912, United States

## S Supporting Information

**ABSTRACT:** Colloidal nanoparticles prepared by solution synthesis with robust control over particle size, shape, composition, and structure have shown great potential for catalytic applications. However, such colloidal nanoparticles are usually capped with organic ligands (as surfactants) and cannot be directly used as catalyst. We have studied the effect of surfactant removal on the electrocatalytic performance of Pt nanoparticles made by organic solution synthesis. Various methods were applied to remove the oleylamine surfactant, which included thermal annealing, acetic acid washing, and UV-Ozone irradiation, and the treated nanoparticles were applied as electrocatalysts for the oxygen reduction reaction. It was found that the electrocatalytic performance, including electrochemically active surface area and catalytic activity, was strongly dependent on the pretreatment. Among the methods studied here, low-temperature thermal annealing ( $\sim 185\text{ }^{\circ}\text{C}$ ) in air was found to be the most effective for surface cleaning without inducing particle size and morphology changes.

**KEYWORDS:** nanoparticles, organic solution synthesis, surfactant removal, catalysis, oxygen reduction reaction



Recently colloidal nanoparticles from aqueous<sup>1–4</sup> or organic,<sup>5–7</sup> solution synthesis have attracted increasing interest for the development of advanced catalysts. Through controlled nucleation and growth in a homogeneous solution, this method has been demonstrated to be powerful in controlling nanoparticle (NP) size,<sup>6,8–10</sup> shape,<sup>1,11,12</sup> composition<sup>13–15</sup> and structure,<sup>16–19</sup> which has enabled systematic studies of these parameters in catalysis.<sup>5,10,18–21</sup> However, the NPs obtained by solution synthesis are usually capped by organic surfactants and cannot be directly applied as catalysts. For example, in the organic solution synthesis of Pt and Pt-based alloy NPs, oleylamine and/or oleic acid are usually used to stabilize the NPs and control NP sizes and shapes.<sup>11,18,22,23</sup> While these ligands are indispensable in the NP synthesis, they are detrimental for catalysis as they block the access of reactant molecules to the surface atoms. Therefore, it is critical to establish a proper procedure of surfactant removal and surface cleaning, without inducing particle size and morphology changes, for application of colloidal NPs in catalysis.

Here we report a systematic investigation of the effect of surfactant removal on the electrocatalytic performance of Pt NPs prepared by organic solution synthesis. Various methods were applied to remove the oleylamine surfactant, including thermal annealing, acetic acid washing, and UV-Ozone irradiation, and the efficiency of surface cleaning was examined by electrocatalytic studies of the treated catalysts for the oxygen reduction reaction (ORR). The removal of organic surfactants from the NP surface was further confirmed by thermogravi-

metric analysis (TGA) and infrared adsorption spectroscopy (IRAS) studies.

## METHODS

**Synthesis.** For the synthesis of Pt NPs, 50 mg of platinum acetylacetonate ( $\text{Pt}(\text{acac})_2$ ) was dissolved in 10 mL of oleylamine at  $100\text{ }^{\circ}\text{C}$  under Ar flow. After 20 min, a mixture of 0.2 g of borane tributylamine (Aldrich) and 5 mL of oleylamine was added into the solution. The solution temperature was raised to  $120\text{ }^{\circ}\text{C}$  and kept at this temperature for an hour. The solution was then cooled to room temperature, and 30 mL of ethanol was added. The product was collected by centrifugation (8,000 rpm, 6 min). The obtained precipitation was dispersed in hexane for further experiments.

**Catalyst Preparation and Surfactant Removal.** The as-synthesized Pt NPs were washed by ethanol and then dried in vacuum. After that, they were mixed with carbon black (Tanaka,  $\sim 900\text{ m}^2/\text{g}$ ) with a mass ratio of 1:1 in chloroform ( $\text{CHCl}_3$ ) by sonication. The solvent was then evaporated at room temperature in air. The obtained powder was denoted as “untreated” catalyst.

The following treatments were applied to the untreated catalyst for surfactant removal: (1) Thermal annealing. The

Received: January 24, 2012

Published: May 21, 2012



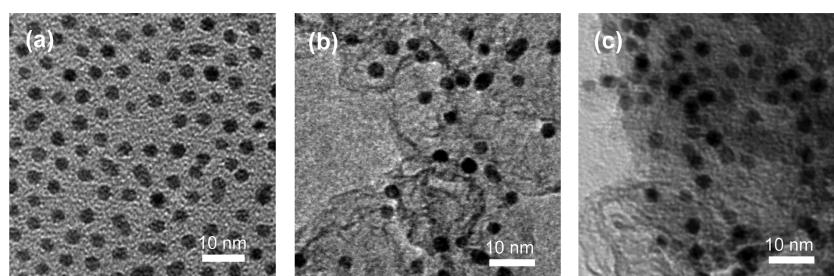


**Figure 1.** TEM images of (a) as-synthesized Pt NPs, (b) Pt NPs loaded on carbon black, and (c) Pt NPs on carbon black after 185 °C annealing.

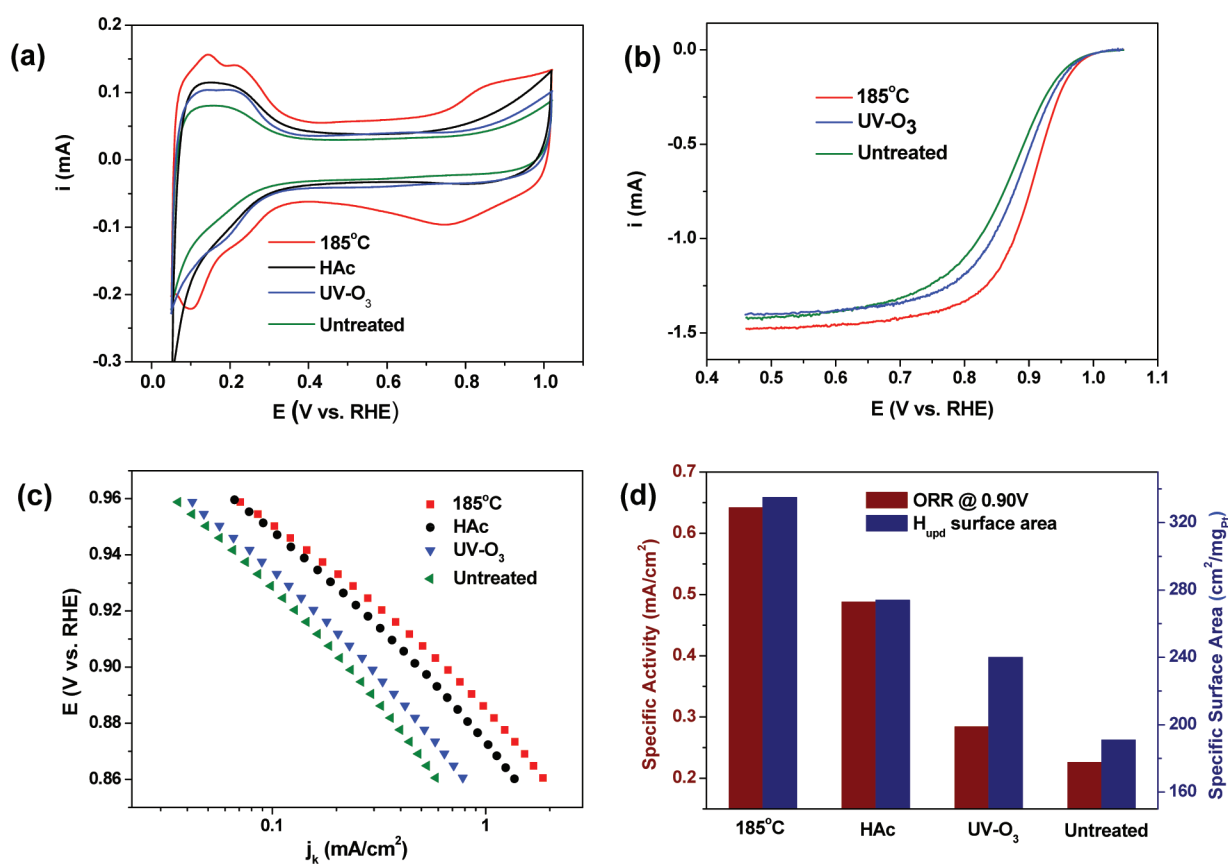


**Figure 2.** (a) Cyclic voltammograms of various Pt/C catalysts. (b) ORR polarization curves of the annealed, the UV-ozone treated and the untreated samples. (c) Tafel plots of Pt/C catalysts at 20 mV/s, 1600 rpm, 20 °C. (d) Specific activity at 0.90 V and specific surface area.

catalyst was heated in a tube furnace for 5 h at 185 °C in air; (2) Chemical washing. The catalyst was dispersed in pure acetic acid (HAc) with vigorous stirring at 75 °C for 10 h, and then collected by adding ethanol and centrifugation; (3) UV-Ozone treatment. An aqueous suspension of the untreated catalyst was deposited onto a glassy carbon electrode. After drying in air, the electrode was placed in a UV-Ozone chamber and subject to UV irradiation for 30 min.

**Characterizations.** Transmission electron microscopy (TEM) images were collected on a Philips EM 30 (200 kV). X-ray diffraction (XRD) patterns were collected on a PANalytical X'pert PRO diffractometer using Cu K $\alpha$  radiation at room temperature. Thermogravimetric analysis for the Pt NPs was done with a Pyris 1 TGA/HT Lab System (PerkinElmer). Fourier transformed infrared (FTIR) spectra were collected on a Nicolet Nexus 8700 spectrometer with a MCT detector cooled by liquid nitrogen and in situ electrode potential control, following the previous reported procedures.<sup>24</sup>

**Electrochemical Studies.** All electrochemical measurements were performed in a three-compartment electrochemical cell in 0.1 M perchloric acid at room temperature. A Ag/AgCl electrode was used as the reference electrode, and a platinum wire as the counter electrode. A mirror-polished glassy carbon disk (6 mm in diameter) was used as the working electrode. The catalyst was dispersed in deionized water by sonication and 30–40  $\mu\text{L}$  of the suspension was deposited onto the glassy carbon electrode by pipet. The loading of Pt was controlled to be  $\sim 20 \mu\text{g}/\text{cm}^2_{\text{disk}}$ . A solution of Nafion (0.1 wt %, 15  $\mu\text{L}$ ) was added on top of the catalyst and then dried in air. Cyclic voltammograms (CVs) were recorded in Ar saturated electrolytes with a scan rate of 50 mV/s. Polarization curves for the ORR were recorded in an oxygen saturated electrolytes at 20 mV/s with an electrode rotation speed of 1600 rpm. All the potentials given were calibrated versus reversible hydrogen electrode (RHE).

## RESULTS AND DISCUSSION

Monodisperse Pt NPs were synthesized by reduction of Pt(acac)<sub>2</sub> with borane tributylamine in an oleylamine solution (see the Methods). Here oleylamine served as both solvent and surfactant. Figure 1a shows a representative TEM image of the as-synthesized Pt NPs with a particle size of  $2.8 \pm 0.4$  nm (Supporting Information, Figure S1a). The synthesized NPs were supported on high-surface-area carbon (Tanaka,  $\sim 900$  m<sup>2</sup>/g) and various treatments were applied to remove the organic surfactants and clean the surface. These include mild-temperature heating (160–200 °C) in air,<sup>25</sup> chemical washing by acetic acid,<sup>26</sup> and UV-Ozone irradiation.<sup>27</sup> No significant change in particle size or morphology was found after these treatments, as shown by the TEM images presented in Figure 1, for example, for the 185 °C thermal treatment in air (Figure 1b,c and Supporting Information, Figure S1b). X-ray powder diffraction patterns of the as-synthesized Pt NPs, 185 °C annealed and HAc treated catalysts were presented in Supporting Information, Figure S2, which shows no significant particle size change or coarsening after these treatments.

Catalytic performance of the various treated catalysts was examined by the RDE method. Figure 2 summarizes the results of electrochemical studies. CVs show typical Pt like features with under potential deposited hydrogen ( $H_{\text{upd}}$ ) peaks at  $E < 0.4$  V (Figure 2a). Among the various treated catalysts, the 185 °C annealed one shows more pronounced  $H_{\text{upd}}$  peaks than the others. As the catalyst loading was consistently controlled to be  $\sim 20$   $\mu\text{g}/\text{cm}^2_{\text{disk}}$ , this difference directly corresponds to the variation in specific surface area, namely, the electrochemically active surface area (ECSA, estimated from the  $H_{\text{upd}}$  charges by  $\text{ECSA} = Q_{H_{\text{upd}}}/210 \mu\text{C}/\text{cm}^2$ ) normalized by the mass of Pt in the catalyst. As shown in Figure 2d, the 185 °C annealed catalyst gave a specific surface area of  $\sim 330$   $\text{cm}^2/\text{g}_{\text{Pt}}$ , versus  $\sim 270$   $\text{cm}^2/\text{g}_{\text{Pt}}$  for the HAc washed,  $240$   $\text{cm}^2/\text{g}_{\text{Pt}}$  for the UV-Ozone treated, and  $190$   $\text{cm}^2/\text{g}_{\text{Pt}}$  for the untreated catalyst. Moreover, the electrocatalytic activity was found to be also strongly dependent on the methods of surfactant removal. Both the polarization curves (Figure 2b) and Tafel plots (Figure 2c) show that the 185 °C annealed catalyst has the highest ORR activity, reaching  $0.64$   $\text{mA}/\text{cm}^2$  at  $0.9$  V, compared to  $0.49$   $\text{mA}/\text{cm}^2$  for the HAc washed,  $0.29$   $\text{mA}/\text{cm}^2$  for the UV-Ozone treated, and  $0.22$   $\text{mA}/\text{cm}^2$  for the untreated catalyst. Both the results of specific surface areas and specific activities indicate that the efficiency of surfactant removal follows the trend 185 °C annealing > HAc washing > UV-Ozone (Figure 2d). It has to be pointed out that potential cycling can bring additional cleaning for the catalysts. For example, after one hundred potential cycles, the HAc washed Pt/C shows comparable electrocatalytic performance as the thermal annealed one (Supporting Information, Figure S3). However, such potential cycling had very limited effect on the UV-Ozone treated and untreated catalysts. In the following discussion, we will focus on the study of surfactant removal by thermal annealing to confirm the effectiveness of surfactant removal.

Figure 3 shows the weight loss curves for the process of surfactant removal by 185 °C annealing in air for the as-synthesized Pt NPs and carbon support. It was found that a weight loss of up to 44% took place during the isothermal process at 185 °C for the NPs, because of the removal of organic surfactants. Not much organic substances were left after the 185 °C stage, as further increase of the temperature up to 900 °C did not lead to substantial loss in addition ( $\sim 1\%$ ). The

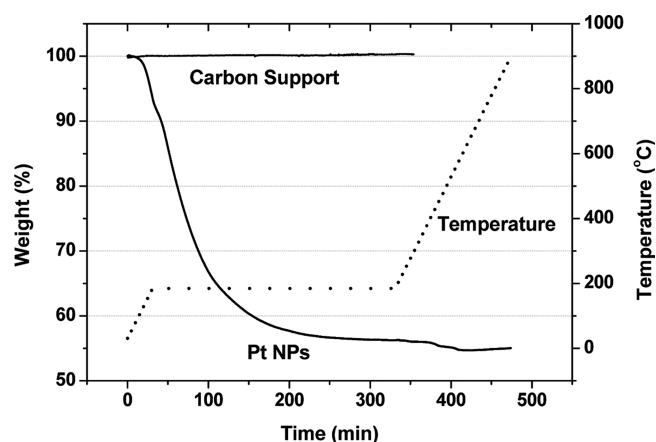


Figure 3. TGA of the as-synthesized Pt NPs and carbon support.

total loss in weight,  $\sim 45\%$ , corresponds to the weight ratio of surfactants in the NPs. On the basis of the TGA studies, we can conclude that the thermal annealing at 185 °C in air is efficient for removing the organic surfactants from the Pt NP surface. It is also important to point out that the employed carbon black is stable in the surfactant removal process, as no weight change was observed in TGA for the carbon support at 185 °C.

After surfactant removal, surface atoms on the Pt NPs were exposed and became electrochemically active. This was further confirmed by in situ electrochemical IRAS studies, in which surface conditions of the NPs as well as the CO-Pt interaction<sup>24</sup> was examined. Figure 4a shows the IR spectra of the annealed and untreated NPs collected at  $0.1$  V in  $0.1$  M  $\text{HClO}_4$  electrolyte. The insets of closeup view highlight the difference between the two spectra in the region from  $2800$   $\text{cm}^{-1}$  to  $3000$   $\text{cm}^{-1}$ . The bands at  $2850$   $\text{cm}^{-1}$  and  $2920$   $\text{cm}^{-1}$  observed in the untreated NPs can be associated to the C–H stretching vibrations in oleylamine molecules.<sup>28</sup> After the thermal annealing, the C–H bands disappeared, suggesting successful removal of surfactants from the particle surface. Figure 4b shows the differentiation spectra obtained by subtracting the IR spectra recorded at  $0.1$  V with the spectra at  $0.9$  V (see Supporting Information, Figure S4 for the primary spectra). Considering that the adsorbed CO ( $\text{CO}_{\text{ad}}$ ) is oxidized at high potentials ( $E = 0.9$  V) while at low potentials CO is strongly adsorbed on Pt, the differentiation spectra are thus able to exclusively tell the situation of CO adsorption on the particle surface. The untreated NPs do not exhibit any observable feature in the wavenumber range from  $1800$   $\text{cm}^{-1}$  to  $2800$   $\text{cm}^{-1}$  because of the blocked CO adsorption on the particle surface. The annealed NPs show a sharp peak at  $2060$   $\text{cm}^{-1}$  which can be assigned to atop-bonded CO on Pt,<sup>29</sup> indicating that the surface atoms were activated by the thermal annealing and became accessible for CO adsorption. The positive peak around  $2340$   $\text{cm}^{-1}$  can be associated with  $\text{CO}_2$  which was the product of CO oxidation. Consistent with the observations from electrochemical and TGA studies (Figure 2 and 3), the IRAS results demonstrate that organic surfactants present on the NP surface, which block  $H_{\text{upd}}$  and CO adsorption and ORR, can be sufficiently removed by the thermal annealing at a mild temperature in air.

## CONCLUSION

We have studied the effect of surfactant removal on the electrocatalytic performance of Pt nanoparticles made by

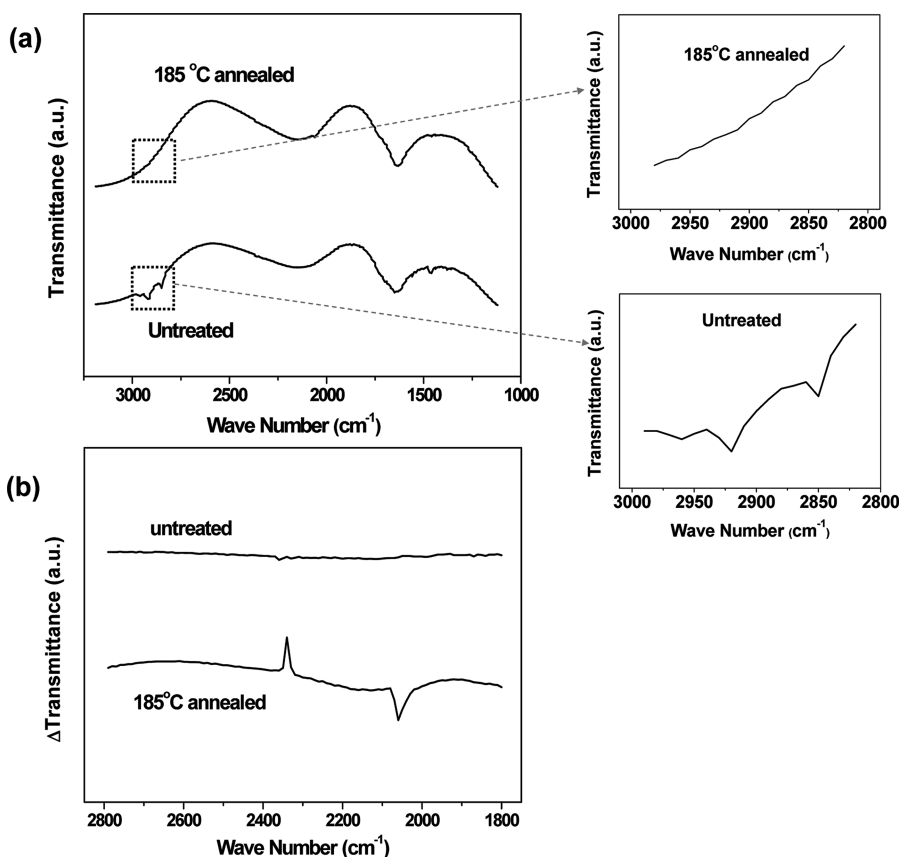


**Figure 4.** (a) FTIR spectra of adsorbed CO on untreated and annealed Pt NPs. The spectra were recorded after CO adsorption at 0.1 V. The insets show the region of the spectra that is typical for surfactant molecules. (b) Subtracted IR spectra at 0.9 and 0.1 V for annealed and untreated samples.

organic solution synthesis. Various methods existing in the literature were applied to remove the oleylamine surfactant, and the dependence of electrocatalytic performance for the ORR on the treatment was found to follow the trend: 185 °C annealing in air > HAC washing > UV-Ozone. The effectiveness of surfactant removal and surface cleaning by thermal annealing in air was further confirmed by TGA and IRAS studies. Our work revealed the importance of pretreatment in catalyst preparation and would have great implication for the development of advanced catalysts with colloidal nanoparticles from solution synthesis.

## ■ ASSOCIATED CONTENT

### Supporting Information

Further details are given in Figures S1–S4. This material is available free of charge via the Internet at <http://pubs.acs.org>.

## ■ AUTHOR INFORMATION

### Corresponding Author

\*E-mail: [ssun@brown.edu](mailto:ssun@brown.edu) (S.S.), [vrstamenkovic@anl.gov](mailto:vrstamenkovic@anl.gov) (V.R.S.).

### Funding

This work was conducted at Argonne National Laboratory, a U.S. Department of Energy, Office of Science Laboratory, operated by UChicago Argonne, LLC, under contract no. DE-AC02-06CH11357. This research was sponsored by the U.S. Department of Energy, Office of Energy Efficiency and Renewable Energy, Fuel Cell Technologies Program. Microscopy research was conducted at the Electron Microscopy Center for Materials Research at Argonne.

## Notes

The authors declare no competing financial interest.

## ■ REFERENCES

- (1) Ahmadi, T. S.; Wang, Z. L.; Green, T. C.; Henglein, A.; El-Sayed, M. A. *Science* **1996**, *272*, 1924–1925.
- (2) Lee, H.; Habas, S. E.; Kweskin, S.; Butcher, D.; Somorjai, G. A.; Yang, P. *Angew. Chem., Int. Ed.* **2006**, *45*, 7824–7828.
- (3) Habas, S. E.; Lee, H.; Radmilovic, V.; Somorjai, G. A.; Yang, P. *Nat. Mater.* **2007**, *6*, 692–697.
- (4) Lim, B.; Jiang, M.; Camargo, P. H. C.; Cho, E. C.; Tao, J.; Lu, X.; Zhu, Y.; Xia, Y. *Science* **2009**, *324*, 1302–1305.
- (5) Wang, C.; Daimon, H.; Lee, Y.; Kim, J.; Sun, S. *J. Am. Chem. Soc.* **2007**, *129*, 6974–6975.
- (6) Tsung, C.-K.; Kuhn, J. N.; Huang, W.; Aliaga, C.; Hung, L.-I.; Somorjai, G. A.; Yang, P. *J. Am. Chem. Soc.* **2009**, *131*, 5816–5822.
- (7) Zhang, J.; Yang, H.; Fang, J.; Zou, S. *Nano Lett.* **2010**, *10*, 638–644.
- (8) Puentes, V. F.; Krishnan, K. M.; Alivisatos, A. P. *Science* **2001**, *291*, 2115–2117.
- (9) Sun, S.; Zeng, H. *J. Am. Chem. Soc.* **2002**, *124*, 8204–8205.
- (10) Wang, C.; van der Vliet, D.; Chang, K.-C.; You, H.; Strmcnik, D.; Schlueter, J. A.; Markovic, N. M.; Stamenkovic, V. R. *J. Phys. Chem. C* **2009**, *113*, 19365–19368.
- (11) Wang, C.; Hou, Y.; Kim, J.; Sun, S. *Angew. Chem., Int. Ed.* **2007**, *46*, 6333–6335.
- (12) Sun, Y.; Xia, Y. *Science* **2002**, *298*, 2176–2179.
- (13) Swafford, L. A.; Weigand, L. A.; Bowers, M. J.; McBride, J. R.; Rapaport, J. L.; Watt, T. L.; Dixit, S. K.; Feldman, L. C.; Rosenthal, S. J. *J. Am. Chem. Soc.* **2006**, *128*, 12299–12306.
- (14) Wang, C.; Chi, M.; Wang, G.; van der Vliet, D.; Li, D.; More, K.; Wang, H.; Schlueter, J. A.; Markovic, N. M.; Stamenkovic, V. R. *Adv. Funct. Mater.* **2011**, *21*, 147–152.

- (15) Chen, W.; Kim, J.; Sun, S.; Chen, S. *J. Phys. Chem. C* **2008**, *112*, 3891–3898.
- (16) Cheng, K.; Peng, S.; Xu, C.; Sun, S. *J. Am. Chem. Soc.* **2009**, *131*, 10637–10644.
- (17) Yavuz, M. S.; Cheng, Y.; Chen, J.; Cobley, C. M.; Zhang, Q.; Rycenga, M.; Xie, J.; Kim, C.; Song, K. H.; Schwartz, A. G.; Wang, L. V.; Xia, Y. *Nat. Mater.* **2009**, *8*, 935–939.
- (18) Wang, C.; van der Vliet, D.; More, K. L.; Zaluzec, N. J.; Peng, S.; Sun, S.; Daimon, H.; Wang, G.; Greeley, J.; Pearson, J.; Paulikas, A. P.; Karapetrov, G.; Strmcnik, D.; Markovic, N. M.; Stamenkovic, V. R. *Nano Lett.* **2011**, *11*, 919–926.
- (19) Wang, C.; Daimon, H.; Sun, S. *Nano Lett.* **2009**, *9*, 1493–1496.
- (20) Lim, B.; Jiang, M.; Camargo, P. H. C.; Cho, E. C.; Tao, J.; Lu, X.; Zhu, Y.; Xia, Y. *Science* **2009**, *324*, 1302–1305.
- (21) Zhang, J.; Yang, H.; Fang, J.; Zou, S. *Nano Lett.* **2010**, *10*, 638–644.
- (22) Sun, S. *Adv. Mater.* **2006**, *18*, 393–403.
- (23) Mazumder, V.; Chi, M.; More, K. L.; Sun, S. *J. Am. Chem. Soc.* **2010**, *132*, 7848–7849.
- (24) Stamenković, V.; Arenz, M.; Ross, P. N.; Marković, N. M. *J. Phys. Chem. B* **2004**, *108*, 17915–17920.
- (25) Liu, Z.; Shamsuzzoha, M.; Ada, E. T.; Reichert, W. M.; Nikles, D. E. *J. Power Sources* **2007**, *164*, 472–480.
- (26) Lee, Y. H.; Lee, G.; Shim, J. H.; Hwang, S.; Kwak, J.; Lee, K.; Song, H.; Park, J. T. *Chem. Mater.* **2006**, *18*, 4209–4211.
- (27) Chen, W.; Kim, J.; Sun, S.; Chen, S. *Phys. Chem. Chem. Phys.* **2006**, *8*, 2779–2786.
- (28) Xu, Z.; Shen, C.; Hou, Y.; Gao, H.; Sun, S. *Chem. Mater.* **2009**, *21*, 1778–1780.
- (29) Chang, S.-C.; Weaver, M. J. *Surf. Sci.* **1990**, *238*, 142–162.